Crystallographic, NMR and *ab initio* calculation studies of tautomerism among substituted dihydrothiazol-2-ylhydrazones

Johan Wouters,†[a] F. Javier Luque,[b] Gloria Uccello Barretta,[c] Federica Balzano,[c] Rosario Pignatello[d] and Salvatore Guccione*[d]

[a] *Fac. Univ. ND de la Paix, 61 Rue de Bruxelles, B-5000, Namur, Belgium. E-mail: johan.wouters@fundp.ac.be; Fax: 32 81 724530*
[b] *Departament de Fisicoquímica, Facultat de Farmàcia, Universitat de Barcelona, Av. Diagonal s/n, S-08028, Barcelona, Spain. E-mail: javier@far1.far.ub.es; Fax: 34 93 4035987; Tel: 34 93 4024557*
[c] *Centro CNR di Studio per le Macromolecole Stereordinate ed Otticamente Attive, Dipartimento di Chimica e Chimica Industriale, Università degli Studi di Pisa, via Risorgimento 35, I-56126, Pisa, Italy. E-mail: gloria@dcci.unip.it; Fax: +39 050 918260; Tel: +39 050 918250*
[d] *Dipartimento di Scienze Farmaceutiche, Facoltà di Farmacia, Università degli Studi di Catania, viale A. Doria 6, Ed. 2, Citta Universitaria, I-95125, Italy. E-mail: guccione@mbox.unict.it; pignatel@mbox.unict.it; Fax: +39 095 443604; Tel: +39 095 738-4020*

Received (in Cambridge, UK) 12th November 2001, Accepted 28th February 2002
First published as an Advance Article on the web 22nd March 2002

The structures of (±)-dihydrothiazolyl hydrazones **3a**,**b** have been fully characterized by combining crystallography, NMR measurements in solution, and computational methods. The thiazolidine structure of the heterocycle is confirmed both by crystallography and in solution. The stability of the endocyclic N3 tautomeric form is confirmed by energy calculation at the MP2/6-31+G(d) level. The *anti-E* conformation observed in the crystal structures is retained in solution, in agreement with stability prediction.

Introduction

Heterocyclic hydrazines and hydrazides have been extensively studied for their potential use as therapeutic agents, in particular for the treatment of hypertension and nervous depression.[1–5] Hydrazono derivatives containing the dihydrothiazole ring (Scheme 1) as the heterocyclic system were fortuitously obtained in an attempt to synthesize hydrazinothiazoles because of an unexpected effect of sodium borohydride in ethanol at 50 °C, with the reduction taking place on the thiazole ring, pharmacological properties of which are well known, instead of the side chain.[1,2,4,5] Actual hydrazinothiazoles were active as monoamine oxidase-B (MAO-B) inhibitors[1–3] whereas the wrongly characterized hydrazonodihydrothiazole *counterparts* were not active against MAO-B. Extensive successful application can make procedures a routine and sometimes cause one to be misled because of a lack of consideration of unexpected effects.[1,2,4,5]

The solid state and solution structures of two selected molecules (Scheme 1), namely 4-ethoxy-3,5-dimethoxybenzaldehyde [4-(4-methoxyphenyl)-4,5-dihydro-1,3-thiazol-2-yl]hydrazone **3a** (reported reaction yield: 72%)[1] and 1,3-benzodioxole-5-carbaldehyde [4-(4-methoxyphenyl)-4,5-dihydro-1,3-thiazol-2-yl]hydrazone **3b** (reported reaction yield: 50%),[1] were established by X-ray crystallography and nuclear magnetic resonance (NMR). The resulting structures suggest an original mechanism of reduction of the azomethine precursors of the dihydrothiazolyl hydrazones. Tautomerism preference within those structures in aqueous solutions was further studied by *ab initio* calculations.

Results

Description of the X-ray structure

A view of the molecular conformation of molecules **3a** and **3b** is given as an ORTEP diagram in Fig. 1. The lattice constants are listed with the relevant crystal data in Table 1. Table 2 lists selected geometric features of both crystal structures.

Molecules **3a** and **3b** crystallise in centrosymmetric space groups, consistent with a racemic (specific [*a*] is 0) composition of the crystals. Both compounds adopt an extended conformation (Fig. 1) with torsion angles N3–C4–N6–N7, C4–N6–N7–C8 and N6–N7–C8–C9 all close to 180°.

Analysis of the bond lengths and angles suggests an sp^3 hybridisation for C1 and C2 and an sp^2 hybridisation for C4, C8, N3, N6, N7. The lengths of carbon–nitrogen bonds C8–N7 and C4–N6 are characteristic of double bonds and significantly shorter than the C4–N3 bond.

H atoms have been located by $F_o - F_c$ (ΔF) Fourier difference maps. A density peak appears close to the N3 nitrogen for structure **3a**, at the end of the refinement, once all heavy atoms are treated anisotropically. The tautomeric N3 form is thus adopted.

The lower quality of the data available for compound **3b** did not allow unambiguous localisation of the H atom on either N3 or N6. Indeed, residual density peaks remained in the $F_o - F_c$ maps close (< 1 Å) to both nitrogens.

In both crystal structures, molecules in the crystal packing are assembled as dimers connected by hydrogen bonds

† *Present address*: Institut de Recherches Microbiologiques Wiame, 1 Av E. Gryzon, B-1070 Brussels, Belgium. E-mail: jwouters@dbm.ulb.ac.be; Fax: 32 2 526 72 73; Tel: 32 2 527 36 34.

 DOI: 10.1039/b110321k

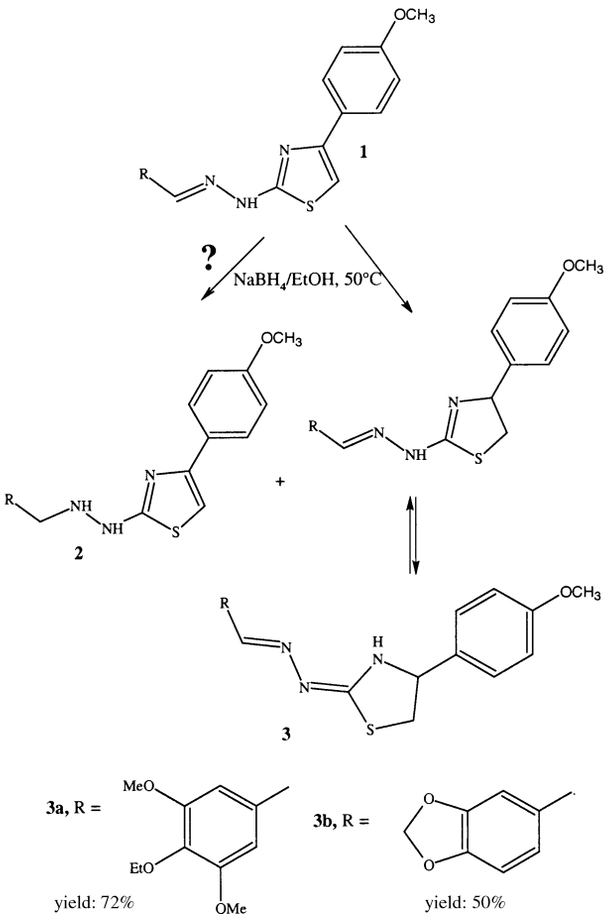

Scheme 1 Chemical structures of azomethine precursors (**1**) and dihydrothiazolyl hydrazones (**2**, **3**) discussed in the text.[1,2,4] Dihydrothiazolyl hydrazones **3** can exist as N3 or N6 tautomers. Experimental conditions and yields of the reactions are described in ref. 1. Subject **3a**, **3b** compounds and related structures coming from the same synthetic procedures were wrongly characterized as the designed corresponding thiazolyl hydrazines,[1] therefore no attempts were made to elucidate whether the two pathways are competitive *i.e.* to detect the actual presence of thiazolyl hydrazines in the reaction mixture (*see the text for explanation*).

(Table 3). An H bond connects endocyclic N3 nitrogen to exocyclic N6 nitrogen. The hydrogen atom, unambiguously located from ΔF Fourier difference maps for **3a**, lies between the two nitrogens, closer to N3. A similar dimeric structure would still be compatible with an N6-H tautomeric structure.

Nuclear magnetic resonance

Compound **3a** has been further characterized in DMSO-d_6 solution by means of ^{1}H and ^{13}C NMR spectroscopy. ^{1}H and ^{13}C chemical shifts data of compound **3a** are collected in Table 4. Its ^{1}H NMR spectrum (Fig. 2) shows well resolved resonances between 8.30 and 1.10 ppm. The high-frequency spectral region contains two singlets at 8.19 and 8.12 ppm; the former is a broad signal due to the proton H3, whereas the latter is produced by the imine proton H4. Three resonances at 7.33, 6.99 and 6.93 ppm are also present, due to pairs of equivalent aromatic protons: their multiplicities confirm the presence of the two different phenyl moieties, 4-methoxy and 3,5-dimethoxy-4-ethoxy substituted. In the low-frequency spectral region, in addition to the expected signals originating from the ether groups bound to the aromatic moieties, three resonances at 4.96, 3.50 and 2.93 ppm are easily distinguishable. Each of them belongs to one proton: the methine proton H2, bound to the carbon bearing the aromatic substituent, and the two diastereotopic geminal protons, H1 and H1′, belonging to the thiazolidine moiety.

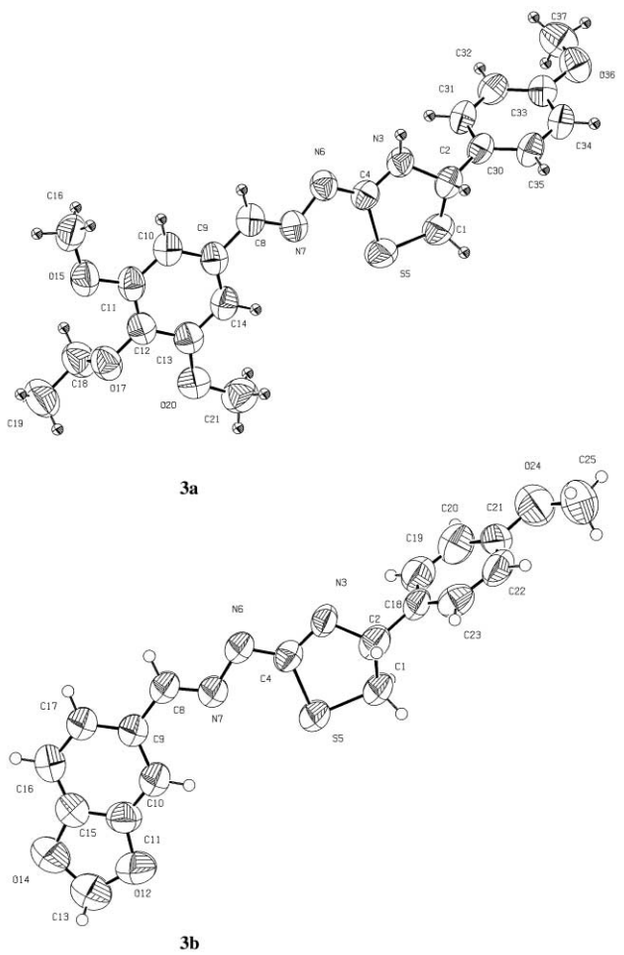

Fig. 1 Structure and solid-state conformation of **3a** and **3b**. Non-H atoms are represented by displacement ellipsoids at the 50% probability level. Atomic numbering of the compounds is provided. For compound **3b**, no H atom could be located on either N3 or N6.

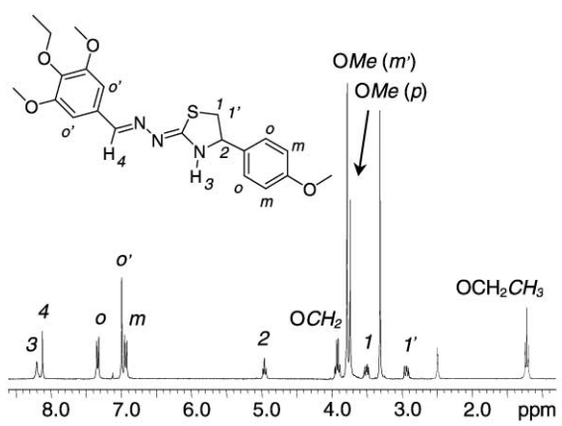

Fig. 2 ^{1}H NMR spectrum (300 MHz, DMSO-d_6, 25 °C) of **3a**.

Accordingly, ^{13}C and ^{13}C-DEPT experiments show eight methyl and methine carbons, six quaternary carbons and two methylene carbons (Fig. 3). In particular, the presence of two CH_2 at 36.7 ppm (endocyclic CH_2) and at 68.6 ppm (OCH_2CH_3) and one CH at 61.3 ppm is a further confirmation of the thiazolidine structure of the heterocycle.

The isomeric/tautomeric structure of the predominant species in solution has been determined by NOE measurements. Indeed, a remarkable dipolar interaction between the H2 and the NH protons (Fig. 4) confirms the presence, as the most abundant species, of the tautomer with the mobile hydrogen located at the endocyclic N3 nitrogen. Concerning the configuration of the hydrazone system, the lack of significant NOE

Table 1 Crystallographic data, data collection and refinement parameters for compounds **3a** and **3b**[a]

	3a	**3b**
Crystallographic data		
Chemical formulae	$C_{21}H_{25}N_3O_4S$	$C_{18}H_{16}N_3O_3S$
Formula weight	415.5	354.4
Crystal system	Monoclinic	Triclinic
Space group	$P2_1/c$	P-1
a/Å	5.894(1)	6.261(1)
b/Å	37.138(6)	8.480(2)
c/Å	9.730(2)	16.433(3)
α/°	90	86.75(3)
β/°	91.83(2)	82.94(3)
γ/°	90	81.98(3)
V/Å^3	2128.7(7)	856.7(7)
Z	4	2
μ[b]/mm^{-1}	1.618	0.211
Data collection		
Temperature/K	293(2)	100(2)
Reflections collected	6512	4268
Independent reflections	4184	2189
R(int)	0.064	0.0226
Observed data [$I > 2\sigma(I)$]	2222	1658
Data refinement		
Final $R1$ [$I > 2\sigma(I)$]	0.0490	0.0838
Final $R1$ (all merged data)	0.1144	0.0994
S = GooF	1.024	1.055
$wR2$	0.1226[c]	0.2375
$\Delta\rho_{max}$	0.176	0.784
$\Delta\rho_{min}$	−0.179	−0.341

[a] Atomic scattering factors from International Tables Vol. C, Tables 4.2.6.8 and 6.1.1.4. [b] Cu-Kα and Mo-Kα for **3a** and **3b** respectively. [c] w = calc $w = 1/[\sigma^2(F_o^2) + (0.0614P)^2 + 0.2261P]$ and w = calc $w = 1/[\sigma^2(F_o^2) + (0.1812P)^2 + 0.2153P]$ where $P = (F_o^2 + 2F_c^2)/3$ for **3a** and **3b** respectively.

Table 2 Selected bond lengths (Å), valence angles (°), and torsion angles (°) for compounds **3a** and **3b**. Esd's are given in parentheses

	3a	**3b**
Bond lengths		
C1–C2	1.522(5)	1.520(7)
C2–N3	1.464(4)	1.472(6)
N3–C4	1.342(4)	1.350(5)
C4–N6	1.294(3)	1.304(5)
N6–N7	1.391(3)	1.393(5)
N7–C8	1.268(4)	1.274(5)
C8–C9	1.459(4)	1.449(6)
Valence angles		
C1–C2–N3	104.2(2)	104.3(4)
C2–C1–S5	107.2(2)	106.7(3)
C2–N3–C4	115.0(2)	113.5(3)
N3–C4–N6	123.9(3)	124.2(4)
C4–N6–N7	110.2(2)	109.9(4)
N6–N7–C8	115.9(2)	116.2(4)
N7–C8–C9	122.3(3)	121.1(4)
Torsion angles		
N3–C4–N6–N7	174.5(2)	178.7(4)
C4–N6–N7–C8	−174.6(2)	−175.7(4)
N6–N7–C8–C9	177.0(2)	179.3(4)
N7–C8–C9–C10	179.4(3)	7.1(7)
N3–C2–C30–C31	−34.2(4)	—
N3–C2–C18–C23	—	137.7(4)

between aromatic protons of the 3,4,5-trisubstituted phenyl moiety and both thiazolidine and *p*-methoxyphenyl protons strongly suggests the *E* and *Z* configurations for the C8–N7 and C4–N6 double bonds, respectively.

It should be noted that the proton spectrum also evidences the presence of another species (less than 5%), originating signals at 8.17, 8.10, 7.12, 5.07, 3.65, 3.06 ppm, the intensities of which are too low to allow its structural characterization.

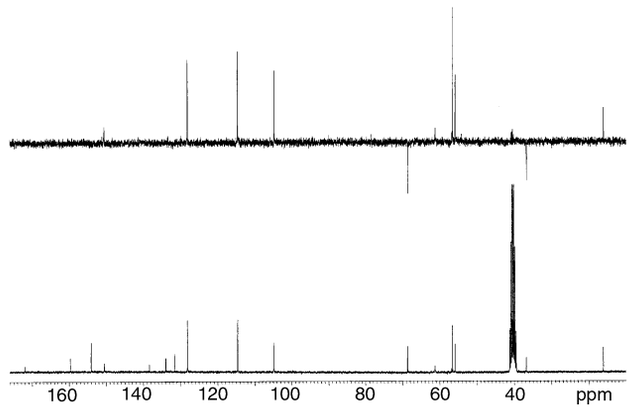

Fig. 3 ^{13}C and ^{13}C-DEPT NMR spectra (75 MHz, DMSO-d$_6$, 25 °C) of **3a**.

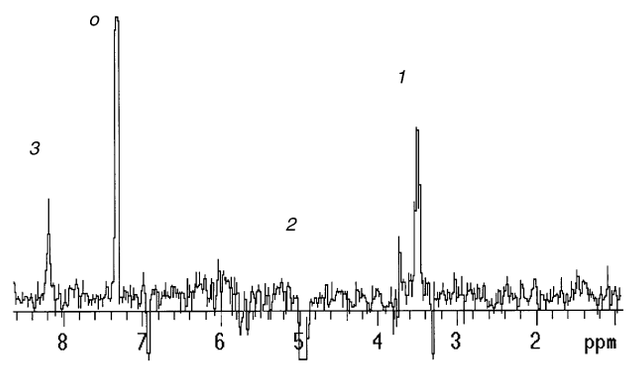

Fig. 4 ^{1}H{^{1}H}-NOE difference spectrum (300 MHz, DMSO-d$_6$, 25 °C) of **3a** corresponding to the saturation of H2.

Ab initio calculations

To complete this study, both tautomeric (N3/N6 tautomerism) and geometric isomeric (*Z*/*E*) preferences were studied in aqueous solution by theoretical calculations. Owing to the large size of the molecules, calculations were performed for structures **a–d** (see Scheme 2) of the thiazolidine model compound **4**.

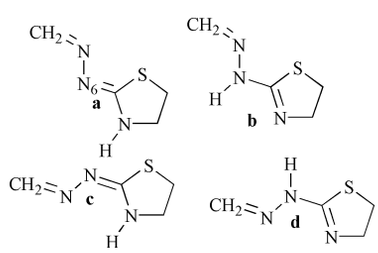

Scheme 2 Simplified structural models (**a–d**) used as input geometries for the *ab initio* calculations of model compounds **4** (thiazolidine) and **5** (thiazole). Both tautomeric (N3/N6 tautomerism) and geometric isomeric (*Z*/*E*) preferences were studied.

To further examine the tautomeric/isomeric properties of this model compound, additional calculations were performed for the thiazole model compound **5**.

Table 5 gives the relative energies computed at the MP2/6-31+G(d,p) level together with the corresponding free energy differences calculated by adding zero-point energy, thermal and entropy corrections to the relative energies in the gas phase. For model compound **4**, species **a** and **c** are the most stable forms in the gas phase, the free energy difference with regard to the other two species being larger than 3.0 kcal mol^{-1}. However, model compound **5** exhibits a clear preference (larger than 5 kcal mol^{-1}) for species **b**.

Table 6 gives the relative values of the free energy of hydration and the estimated free energy difference in water, which was determined by adding the relative hydration free energy to

Table 3 Geometry (Å, °) of hydrogen bonds stabilising the crystal packing of compounds **3a** and **3b**

D–H ··· A	*d* (D ··· A)	*d* (H ··· A)	∠ (DHA)
Compound **3a**			
N3–H ··· N6 ($-x+2, -y, 1-z$)	2.95	1. 98	161
Compound **3b**			
N3–H ··· N6 ($1-x, 1-y, 1-z$)	2.99	2. 25	145

Table 4 ^{1}H and ^{13}C chemical shifts (ppm) data of compound **3a**

Protons	δ (m, *J*)	Carbons	δ
4	8.12 (s)	CH_3CH_2O	16.1
3	8.19 (s)	CH_2	36.7
2	4.96 (dd, 7.5 and 6.9 Hz)	CH_3O (*p*)	55.9
1	3.50 (dd, 11.0 and 6.9 Hz)	CH_3O (*m′*)	56.5
1′	2.93 (dd, 11.0 and 7.5 Hz)	*CH*	61.3
o′	6.99 (s)	CH_3CH_2O	68.6
O*Me* (*m′*)	3.78 (s)	*CH* (*o′*)	104.8
OCH_2CH_3	3.92 (q, 7.0 Hz)	*CH* (*m*)	114.6
OCH_2CH_3	1.22 (t, 7.0 Hz)	*CH* (*o*)	128.1
o	7.33 (d, 8.8 Hz)	*CH*=N	150.5
m	6.93 (d, 8.8 Hz)		
O*Me* (*p*)	3.74 (s)	Quaternary C	131.5, 133.9, 138.3, 154.0, 159.6, 171.9

Table 5 Energy and free energy differences in the gas phase (kcal mol^{-1}) between tautomers/isomers determined at the MP2/6-31+G(d,p) levels for the four species **a–d** for model compounds **4** and **5**

	ΔE(**4**)	ΔG(**4**)	ΔE(**5**)	ΔG(**5**)
a	−4.1	−3.0	+5.1	+5.1
b	0.0	0.0	0.0	0.0
c	−3.5	−3.1	+6.0	+6.1
d	+4.2	+4.2	+6.6	+6.2

Table 6 Relative free energy of hydration (ΔG_{hyd}) and free energy differences (ΔG_{wat})[a] in aqueous solution (kcal mol^{-1}) between the four species **a–d** for model compounds **4** and **5**

	ΔG_{hyd}(**4**)	ΔG_{wat}(**4**)	ΔG_{hyd}(**5**)	ΔG_{wat}(**5**)
a	−0.3	−3.6	−1.3	+3.8
b	0.0	0.0	0.0	0.0
c	+0.5	−2.3	−0.4	+5.7
d	−3.1	+1.2	−3.6	+2.6

[a] Determined by adding the relative hydration free energy to the gas phase free energy difference computed at the MP2/6-31+G(d,p) level of theory.

the gas phase (MP2/6-31+G(d,p)) free energy difference. For the two compounds, hydration stabilises preferentially species **d**, but this effect is not large enough to revert the relative stability in the gas phase. Thus, calculations predict species **a** and **c** to be the preferred forms in aqueous solution for model compound **4** (thiazolidine), and species **b** for model compound **5** (thiazole).

Discussion

Analysis of the bond lengths and angles reveals an sp^3 hybridisation for C1 and C2 and an sp^2 hybridisation for C4, C8, N3, N6, N7. Reduction of compounds **1** (Scheme 1) by $NaBH_4$ under the conditions described by Mazzone *et al.*[1] thus leads to isomers **3** and not **2** (Scheme 1).

The geometry deduced from the crystal structure analysis and the observation of an hydrogen atom on the endocyclic N3 nitrogen in the ΔF map, for **3a**, is in favour of the N3 tautomeric form for dihydrothiazolyl hydrazones. This structure of dihydrothiazolyl hydrazones is also observed in solution. The thiazolidine structure of the heterocycle is confirmed by the analysis of ^{1}H and ^{13}C chemical shifts: endocyclic carbons C1 (CH_2) and C2 (CH) appear in the ^{13}C spectra at 36.7 and 61.3 ppm, respectively. In the ^{1}H spectrum, protons on C1 (H1 and H1′) come out at 3.50 and 2.93 ppm while the methine proton on C2 (H2) is at 4.96 ppm. This last proton strongly interacts with the NH proton as deduced by NOE measurements, confirming the presence of the tautomer with the mobile hydrogen located at the endocyclic N3 nitrogen. Therefore, it appears that the structure of **3a** in solution is similar to the geometry observed in the crystal structure.

Theoretical studies of the tautomerism/isomerism preferences of dihydrothiazolyl hydrazones **3a**,**b** have been performed by calculating the energy differences and relative hydration free energies of model compounds **a**, **b** (Scheme 2). The *ab initio* calculations (Tables 5 and 6) clearly indicate that the relative stability in the gas phase is little affected upon hydration. According to the results for model compound **4**, the populations of the four species in aqueous solution are predicted to be 90%, <1%, ~10% and <1% for **a**, **b**, **c**, and **d**, respectively. This prediction is in complete agreement with the experimental structure of **3a** observed both by crystallography in the solid state and by NMR in solution. In contrast, calculations predict that species **b** is the most stable form in aqueous solution for model compound **5** (thiazole).

Conclusions

The structures of the dihydrothiazolyl hydrazones **3a**,**b** (Scheme 1) obtained by reduction of the azomethine precursor under the conditions described by Mazzone *et al.*[1] have been fully characterised by combining crystallography, NMR measurements in solution, and computational methods. The thiazolidine structure of the heterocycle is confirmed both by crystallography and in solution. The stability of the endocyclic N3 tautomeric form (**a**, Scheme 2), in the gas phase and in water, is confirmed by energy calculation at the MP2/6-31+G(d) level. This tautomeric structure is expected to be the most abundant form (>90%) of the molecule.

The *anti-E* conformation observed in the crystal structures is retained in solution, in agreement with stability prediction.

Synergy between theoretical and experimental data has proven to be a very powerful tool to elucidate shape and subshape properties (spatial arrangement of putative *pharmacophore* groups) as a consequence of a different conformational freedom which can produce *enantiotopy* also within closely related structures. Obviously, considering the substantial role electronic factors play in the MAO action, the different electronic character can also affect the anti-MAO activity.

These findings can be exploited both to support pharmacophoric hypotheses[4] in the drug design of high affinity and selective MAO inhibitors as potential drugs and to be used as probes to map the monoamine oxidases-A and -B active site structure. The latter was recently reported by Mattevi and Edmonson *et al.*[12] Moreover, the rationale elucidating the alternate synthetic pathway leading to the *unexpected* thiazolidine derivatives can lead to selective synthesis with improved yields of these thiazolidines or their unsaturated *counterparts* if the two pathways should be competitive. Further studies will be carried out to separate the racemic mixture considering the influence of stereochemical aspects in the specific binding of MAO-A or -B and thus to define the role of each thiazolidine enantiomer as *bioactive* or *ballast* and to make a comparison with the unsaturated *counterpart*, *i.e.* with similarly substituted hydrazinothiazole derivatives[1–4] taking advantage of the recently reported MAO-B structure.[12]

Experimental

Synthesis

4-Ethoxy-3,5-dimethoxybenzaldehyde [4-(4-methoxyphenyl)-4,5-dihydro-1,3-thiazol-2-yl]hydrazone **3a** and 1,3-benzodioxole-5-carbaldehyde [4-(4-methoxyphenyl)-4,5-dihydro-1,3-thiazol-2-yl]hydrazone **3b** were prepared according to Mazzone *et al.*[1] As our aim was only to check the reaction was reproducible no attempts were made to improve the yields.

X-Ray crystallography ‡

Crystals of compounds **3a** and **3b** were obtained by slow evaporation of concentrated solutions in low molecular weight alcohols.

A suitable crystal of **3a** was mounted on a quartz fiber on a goniometer head of a CAD4 Nonius diffractometer. After determination of the cell parameters using 25 well centered reflections, a complete diffraction data set was collected. Analytical correction for absorption was introduced.

Only small crystals of **3b** could be grown. Therefore diffraction data were collected for this compound using a rotating anode Rigaky diffractometer and a MAR Image Plate detector.

After intensity integration and data corrections the structures were solved using direct methods and refined by full matrix least squares on F^2 using the program SHELXL97.[6] All non hydrogen atoms were treated anisotropically while a riding model was applied for the hydrogens. The positions of the hydrogens were obtained from careful inspection of Fourier difference ΔF maps.

Nuclear magnetic resonance

All spectra were recorded using a spectrometer operating at 300 and 75 MHz for ^{1}H and ^{13}C, respectively and the temperature was controlled to ±0.1 °C. All ^{1}H and ^{13}C NMR chemical shifts are referenced to TMS as external standard. ^{13}C DEPT (Distortionless Enhancement by Polarisation Transfer) spectra were obtained for a spectral width of 16000 Hz, collecting 32K data points. The 90° pulse was 13.2 μs, the proton pulse was 12.0 μs and the $(2J)^{-1}$ delay was set equal to 3.57 ms.

The ^{1}H{^{1}H}-NOE (Nuclear Overhauser Effect) experiments were performed in the difference mode. The decoupler power used was the minimum required to saturate the spin of interest. A waiting time of 5–10 s was used to allow the system to reach equilibrium. Each NOE experiment was repeated at least four times. All the solutions were accurately degassed by freeze–pump–thaw cycles for NOE experiments.

‡ CCDC reference numbers 174656 and 174657. See http://www.rsc.org/suppdata/p2/b1/b110321k/ for crystallographic files in .cif or other electronic format.

Ab initio calculations

Geometry optimisations were performed at the HF level using the 6-31G(d) basis[7] on simplified structure to reduce the computing time. The minimum energy nature of the stationary points was verified from the harmonic frequency analysis. Single-point calculations were performed at the second-order Moller–Plesset[8] (MP2) with the 6-31+G(d,p) level using the HF/6-31G(d) optimised geometry. The HF/6-31G(d) vibrational frequencies were used to compute zero-point energy thermal and entropy corrections (at 298 K), in order to estimate free energy differences between tautomers. Gas phase calculations were performed using Gaussian-94.[9]

Calculations in solution were performed using the HF/6-31G(d) parameterised version of the MST model[10] implemented in MONSTERGAUSS.[11] Addition of the free energies of solvation to the gas phase free energy differences allows us to compute the relative stability of tautomers in water.

Calculations were carried out on SGI Octane R-12000 and R-5000 workstations operating under IRIX 6.5.+.

Specific rotation

The zero specific rotation $[\alpha]_D$ due to the racemic mixture was determined on 10 mg of substance with a JASCO DIP-135 polarimeter in DMSO as the solvent at 25 °C.

Acknowledgements

We thank Bernadette Norberg for her help with crystallisation and data collection. We are grateful to Professor J. Tomasi for providing his original code of the PCM model, which was modified to carry out the MST calculations and Professor V. Amico for providing the specific rotation value $[\alpha]_D$. We also acknowledge the Dirección General de Investigación Científica y Técnica (grant PB98-1222) for financial support.

References

1 G. Mazzone, R. Pignatello, A. M. Panico, S. Mazzone, G. Puglisi, G. Pennisi, G. Raciti, P. Mazzone and M. Matera, *Pharmazie*, 1992, **47**, 902–910.
2 G. Raciti, P. Mazzone, P. A. Raudino, G. Mazzone and A. Cambria, *Bioorg. Med. Chem.*, 1995, **3**, 1485–1491 and references therein enclosed.
3 A. Cambria, A. Raudino, F. Castelli, G. Raciti, P. Mazzone, G. Buemi, R. Pignatello and G. Mazzone, *J. Enzyme Inhib.*, 1996, **10**, 215–229.
4 S. Gritsch, S. Guccione, R. Hoffman, A. Cambria, G. Raciti and T. Langer, *J. Enzyme Inhib.*, 2001, **16**, 199–215.
5 J. Wouters, B. Norberg and S. Guccione, *Acta Crystallogr., Sect. C*, 2001, **57**, 69–71.
6 G. M. Sheldrick and T. R. Schneider, *SHELXL: High Resolution Refinement*; ed. R. M. Sweet and C. W. J. Carter, Academic Press, Orlando, Florida, 1997, vol. 277, pp. 319–343.
7 P. C. Hariharan and J. A. Pople, *Theor. Chim. Acta*, 1973, **28**, 213.
8 C. Møller and M. S. Plesset, *Phys. Rev.*, 1934, **46**, 618.
9 M. J. Frisch, G. W. Trucks, H. B. Schlegel, P. M. W. Gill, B. G. Johnson, M. A. Robb, J. R. Cheeseman, T. A. Keith, G. A. Petersson, J. A. Montgomery, K. Raghavachari, M. A. Al-Laham, V. G. Zakrzewski, J. V. Ortiz, J. B. Foresman, J. Cioslowski, B. B. Stefanov, A. Nanayakkara, M. Challacombe, C. Y. Peng, P. Y. Ayala, W. Chen, M. W. Wong, J. L. Andres, E. S. Replogle, R. Gomperts, R. L. Martin, D. J. Fox, J. S. Binkley, D. J. Defrees, J. Baker, J. P. Stewart, M. Head-Gordon, C. Gonzalez and J. A. Pople, Gaussian 94. Rev. A.1, Gaussian Inc., Pittsburgh, 1995.
10 C. Curutchet, M. Orozco and F. J. Luque, *J. Comput. Chem.*, 2001, **22**, 1180.
11 M. Peterson and R. Poirier, *MonsterGauss*, Department of Biochemistry, University of Toronto, Canada. Version modified by R. Cammi and J. Tomasi (1987) and by F. J. Luque and M. Orozco (2000).
12 C. Binda, P. Newton-Vinson, F. Hubálek, D. E. Edmondson and A. Mattevi, *Nature Struct. Biol.*, 2002, **9**, 22–26. Published online November 26, 2001.